International Journal of Engineering, Science and Mathematics
Vol.11 Issue 11, November 2022,
ISSN: 2320-0294 Impact Factor: 6.765
Journal Homepage: http://www.ijmra.us, Email: editorijmie@gmail.com
Double-Blind Peer Reviewed Refereed Open Access International Journal - Included in the International Serial Directories Indexed & Listed at: Ulrich's Periodicals Directory ©, U.S.A., Open J-Gage as well as in Cabell's Directories of Publishing Opportunities, U.S.A

Non-Linear Behaviour of Laterally Loaded Flexible Piles in Cohesionless Soil

Gururaj M. Vijapur*
B.S.Chawhan**

Abstract

Data were taken during the lateral loading of single 600mm diameter test pile installed at a site where the soils consisted of clean fine cohesionless soil to silty fine cohesionless soil. Two types of loading were employed, static loading and cyclic loading. The data were analyzed and families of curves were developed which showed the soil behavior presented in terms of the lateral soil resistance *p* as a function of pile deformation *y*. With theoretical studies as a basis, a method were derives for predicting the family of *p-y* curves based on the properties of cohesionless soil and pile dimensions. Procedures are suggested for both static loading and cyclic loading. While there is some basis for the methods from theory, the behavior of cohesinless soil and around a laterally loaded pile does not yield to a completely rational analysis therefore, a considerable amount of empiricism is involved in the recommendations. The procedure was employed for predicting *p-y* curves at the experimental site and computed results are compared with experimental results. The agreement is good.

Keywords:

Static load;
Cyclic load;
p-y curves;
Lateral loading;
Pile deformation.

Author correspondence:

Gururaj M. Vijapur,
Assistant Professor, Civil Engineering Department,Government Engineering College, Haveri, Karnataka, India-581110.
vijapur2022@gmail.com

1. Introduction

There are a relatively small number of papers in the technical literature which give recommendations for predicting the behaviour of the soil around the piles subjected to lateral loading. With regard to cohesionless soil, such recommendations are made in two papers, Terzaghi and Parker and Reese [2]. Terzaghi presents no experimental; the paper by Parker and Reese is based on lateral load tests of small diameter piles. The method presented below is based on the results of full-scale tests of instrumented piles and should be a useful addition to the literature. The differential equation, Eq.1, for the problem of the laterally loaded pile is well known and its solution has been discussed by a number of authors [3.4.5.6.7].

$$EI\frac{d^4y}{dx^4}+E_s y=0 \quad \text{----------(1)}$$

where,

*Assistant Professor, Civil Engineering Department, Government Engineering College, Haveri, Karnataka, India-581110.
**Assistant Professor, Civil Engineering Department, Government Engineering College, Haveri, Karnataka, India-581110.

y=deformation, x=length along pile, EI=flexural stiffness of pile and E_s=soil modulus.
It should be noted that, Eq. 1 does not include a term to account for the effect of axial load on bending. If the axial load is suitable, Eq.1 should be expanded.

As indicated in the referenced papers, appropriate solutions can sometimes be obtained by the use of non-dimensional relationships. A more favourable approach is to write the differential equation in difference form and to obtain solutions by use of the numerical techniques (Software package).

In the solution of the differential equation, appropriate boundary conditions must be selected at the top of the pile to insure that the equations of equilibrium and of compatibility are satisfied at the interface between the pile and the superstructure. The selection of the boundary conditions is a simple problem in some instances; for example, where the superstructure is simply a continuation of the pile. However, in other instances, it may be necessary to alternate between solutions for the piles and for the superstructure in order to obtain a correct solution. Such iteration may be required because the soil behaviour is usually non-linear.

2. Literature Review

The thrust of most of the recent research on laterally loaded piles has been at the development of curves giving the soil resistance *p* as a function of the pile deformation *y*. A recent well-known paper by Matlock [8] presents a procedure for the development of *p-y* curves was first developed by McClelland and Focht [9]. While other procedures have been suggested for the design of piles under lateral loadings, most designers favour the use of the *p-y* curves, because it is the most rational procedure yet suggested.

Byung, Nak-Kyung et al. [19]have observed that, experimental load-transfer curves are determined with scaling factors to take into account the effects of pile installation method and the pile head restraint condition were studied. The relation of the soil-pile reaction of the fixed head condition to the free head condition was the highest near the soil surface and decreases as the depth increases. ShamsherPrakash and Sanjeevkumar [20]have concluded that, a given relative density of sand, the modulus of subgrade reaction is an experimental function of strain. Modulus of horizontal subgrade reaction depends strongly of the relative density of sand and position of the ground water table. Chandrasekaran et al. [21] have investigated that, the effects of pile spacing, number of piles, embedment length and configuration on pile-group interaction. From the experimental results, it has been found that the lateral capacity of piles in nine pile group at three-diameter spacing is about 40% less than that of the single pile and causes 20% increase in the maximum bending moment when compared with single pile.

Sundaravadivelu [22] reported the analysis of laterally loaded pile in soft clay, idealising the pile as beam element and the soil by non-linear inelastic spring element, modelled with elasto-plastic sub elements. An iterative procedure was adopted to perform a non-linear finite element analysis and the effect of static lateral load on load-deformation behaviour was studied. Rathod et al. [23]have investigated that, the effect of slope on *p-y* curves for laterally loaded piles in soft clay. The results show that the pile top displacement and the bending moment in the pile decrease with an increase in the slope. An increase in the ground slope causes an increase in the pile displacement and bending moments at any depth of the pile.

3. Soil Behaviour Defined by Family of *p-y* Curves

The idea of *p-y* curves is presented in Fig.1. Figure 1 shows a section through a pile at depth below the ground surface. The behaviour of a thin stratum of soil at a depth x_1 below the ground surface will be discussed. Fig.1(b) shows a possible earth pressure distribution around the pile after it has been installed and before the pile after it has been installed and before the pile has been loaded laterally. The earth pressure distribution in Fig.1(b) assumed that the pile was perfectly straight prior to driving and that there was no bending of the pile driving.

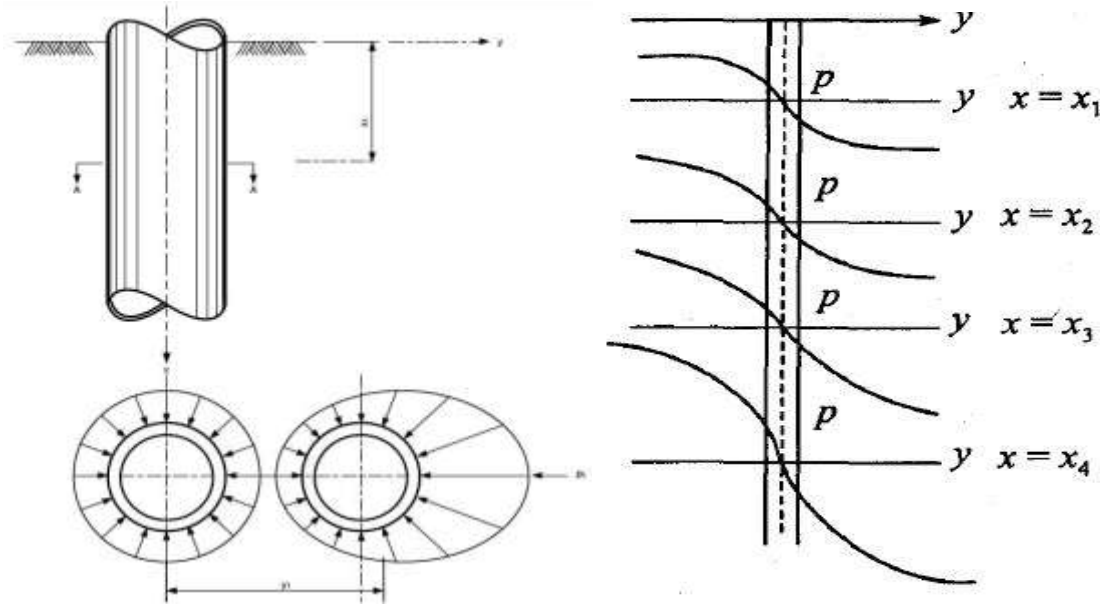

(a) *(b)*

Fig.1(a) Definition of soil response curve, b. Soil response curves by depths.

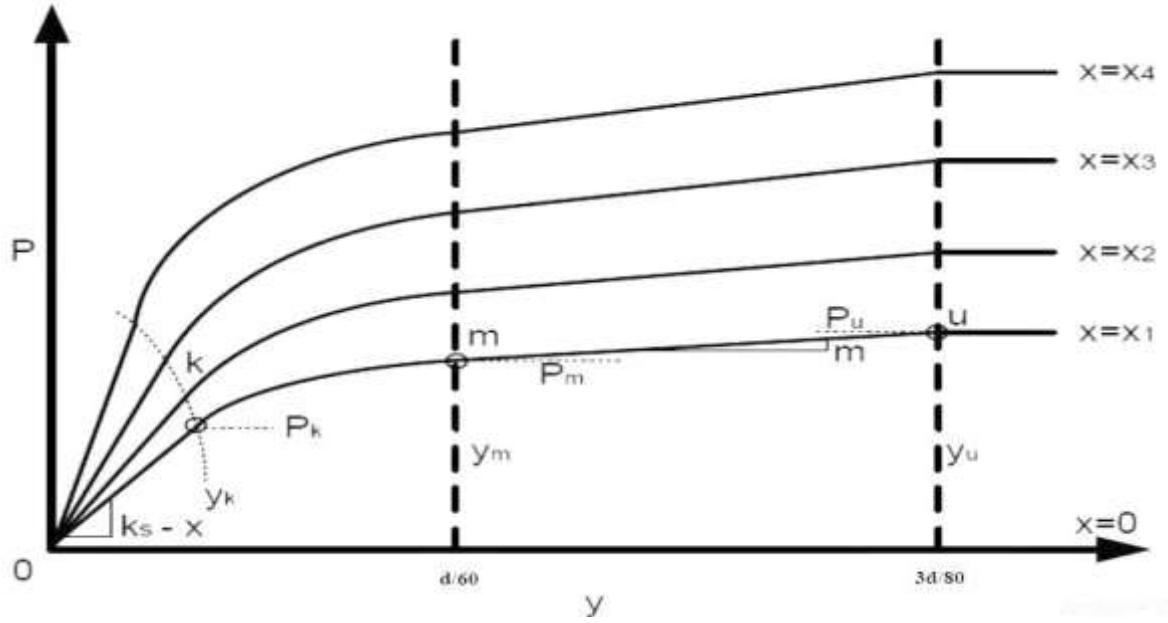

Fig.1(c) Characteristic shape of a family of p-y curves for static and cyclic loading in cohesionless soil

While neither of these conditions is precisely met in practice. It is believed that in most instances the assumptions can be made without serious error. The deformation of the pile through a distance $y_1$as shown in Fig.1(c), would generate unbalanced soil pressures against the pile, perhaps as indicated in the figure. Integration of the soil pressures around the pile would yield an unbalanced force p_1 per unit of length of the pile.The deformations of the pile could generate a lateral soil resistance parallel to the axis of the pile; however, it is assumed that such lateral soil resistance would be quite small and it can be ignored in the analysis.

As shown in Fig.1(a), the deformation of $y_1$is the distance the pile deflects laterally on being subjected to a lateral load. The lateral soil resistance p_1 is the force per unit length from the soil against the pile which develops as a result of the pile deformation.

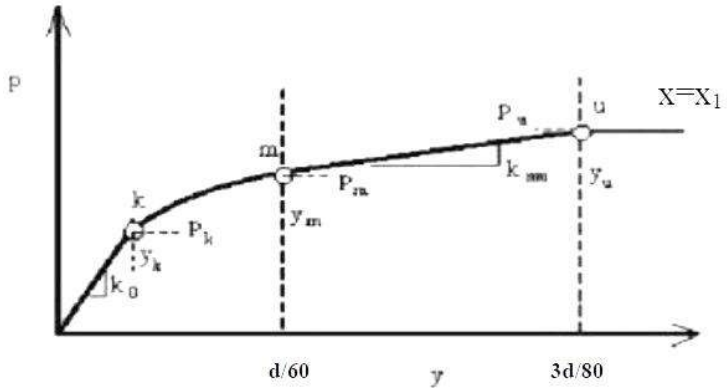

Fig.2 Construction of p-y curve

For the solution of the problem of a laterally loaded pile, it is desirable to be able to predict a set of *p-y* curves, such as those shown in Fig.2. If such a set of curves can be predicted, Eq.1 can readily be solved to yield pile deformation, pile rotation, bending moment, shear, and soil reaction for any load capable of being sustained by the pile.

The set of curves shown in Fig.2 would seem to imply that the behaviour of the soil at a particular depth is independent of the soil behaviour at all other depths. That assumption, of course, is not strictly true. However, it has been found by experiment [8] that, for the pattern of pile deformations which can occur in practice, the soil reaction at a point is dependent essentially on the pile deformation at that point and not on pile deformations above and below. Thus, or purposes of analysis, the soil can be removed and replaced by a set of discrete mechanisms with load-deformation characteristics of a character such as shown in Fig.2.

4. Brief Description of Experiments

The experiments from which this paper is based are described in detail in a companion paper [11]. Briefly, the experiments entailed the application of known lateral loads in the field to full-sized piles, which were instrumented for the measurement of bending moment along the length of the piles. In addition to the measurement of the load at the ground line, measurements were made of pile-head deformation and pile-head rotation. Two types of loading were employed, static and cyclic.

Single pile was driven open-ended at the test site on Verda River near Haveri, Karnataka, INDIA. The water table was maintained above the ground surface during loading to simulate conditions which would exist at an offshore location.

For each type of loading, a series of lateral loads were applied, bending with a load of small magnitude. A bending moment curve was obtained for each load; thus, the experiments resulted in a set of bending moment curves, along with the associated boundary conditions or each type of loading.

Soil studies were made at the site involving the use of undisturbed sampling. Laboratory studies were performed. The cohesionless soil at the test site varied from clean fine cohesionless soil to silty fine cohesionless soil, both having high relative densities. The cohesionless soil particles by inspection through a microscope were found to be sub angular with a large percentage of flaky grains. The angle of internal friction Φ was determined to be 39 degrees and the value of the submerged unit weight γ′ was found to be 10.40kN/m^3.

4.1 Determination of Soil Behaviour from Experimental Results

From the sets of experimental bending moment curves described above, values of *p* and *y* at points along the pile can be obtained by solving the following equation:

$$y = \iint \frac{M(x)}{EI} \quad \text{----------(2)}$$

$$p = \frac{d^2 M(x)}{dx^2} \quad \text{----------(3)}$$

Appropriate boundary conditions must be used and the applications must be solved numerically.

The solution of Eq.2 for values of *y* can normally be accomplished with appropriate accuracy. However, analytical difficulty is encountered in the solution of Eq.3. If extremely accurate moment values are available, the double differentiation can be performed numerically [12]. The procedure employed for obtaining the lateral soil resistance curves in this study involved the prior assumption that the soil modulus could be described as a function of depth by a two-parameter, nonlinear curve. The two parameters were

computed from the experimental data, allowing the soil reaction curve to be computed analytically. The procedure has been described in detail in a previous paper [10].

5. Theoretical Basis for Soil Behaviour

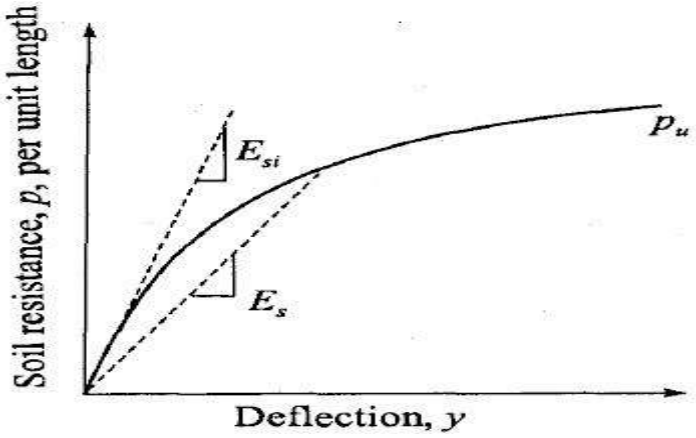

Fig.3 Characteristic shape of a p-y curve

A typical *p-y* curve is shown in Fig.3. The curve is plotted in the first quadrant for convience. As may be noted in the figure, the initial portion of the curve is essentially a straight line, as defined by the modulus E_{s1}. This portion of the curve can be thought to represent the linear elastic behaviour of the soil, and could possibly be derived theoretically if solutions were available from the theory of elasticity. Terzaghi [1] suggested numerical values for E_{s1} as a function of the unit weight and the relative density of cohesionless soil. He suggested that E_{s1} is zero at the ground surface and increases linearly with depth; his suggestion was based on the fact that experiments had shown that the initial slope of a laboratory stress-strain curve for cohesionless soil is a linear function of the confining pressure.

In this paper, no attempt is made to derive by rigorous theory numerical values for the initial slope of the *p-y* curve; rather, the slope of that portion of the curve is established on the basis of experiments which were performed. However, theory is employed to the extent that the slope of the initial portion of the curve E_{s1} is given by the following equation:

$$E_{s1} = N_h x \quad \text{----------} \quad (4)$$

where,

N_h=a coefficient of soil modulus variation in kN/m^3

x=depth below ground surfacein meter

The values of N_h recommended by Terzaghi are shown in Table1. The values of N_h obtained from the Verda River cohesionless soil test for the static case were 2.5 times the highest value reported by Terzaghi. The values for the cyclic case were 3.9 times the highest value given by Terzaghi. With regard to recommended values. It is proposed that the values of N_h shown in Table 2 be used. These values of N_h are recommended for static and cyclic loading.

Table 1.Terzaghi's values of N_h for submerged sand

Relative Density	Loose	Medium	Dense
Range of value of A	100-300	300-1000	1000-2000
Adopted value of A	200	600	1500
Range of values of N_h in kN/m^3	706-2090	2090-7057	7057-13843

Table 2.Terzaghi's values of N_h for submerged sand (static and Cyclic loading)

Relative Density	Loose	Medium	Dense
Range of value of A	100-300	300-1000	1000-2000
Range of values of N_h in kN/m^3	5428	16286	33929

An examination of the shape of the *p-y* curves which are recommended see Fig.3 shows that the initial straight-line portions of the curves where E_s is linear with deformation governs for only small deformations.

Therefore, the initial slope of the *p-y* curve influences analysis only for the very smallest loads. In more normal cases a secant modulus, such as the one defined by E_{sn} shown in Fig.3, controls the analysis. Because the initial portion of the *p-y* curve has little influence on most analyses and because of the relatively small amount of data on the early portions of the curves, it was thought to be undesirable to recommend different values of N_h for static and for cyclic loading.

Referring to Fig.3, it may be seen that lateral soil resistance *p* attains a limiting value defined as the ultimate lateral soil resistance p_u. Soil mechanics theory can be applied to derive equations for p_u for two cases, near the ground surface and at depth.

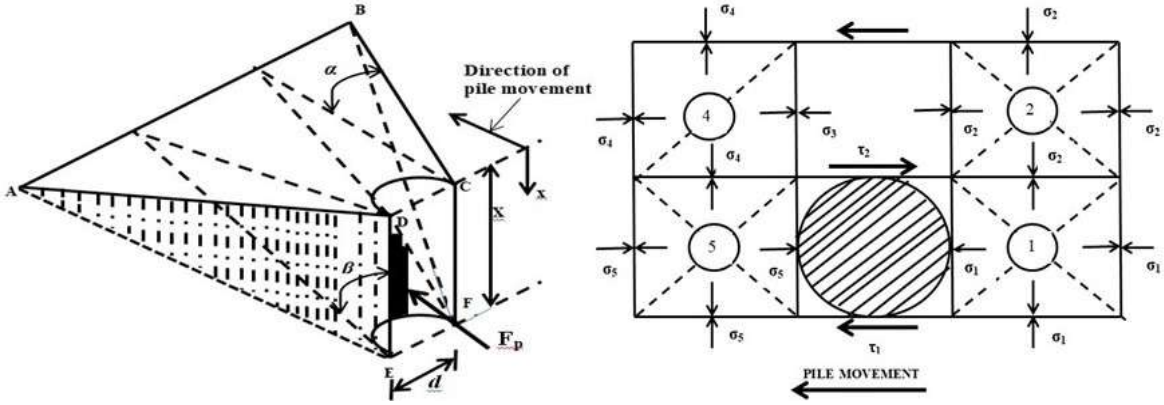

(a). Wedge failure mode *(b). Block failure mode*

Fig.4 Two types of soil failure mode

The ultimate lateral soil resistance near the ground surface is computed using the free body shown in Fig.4. As may be seen in the figure, the total ultimate lateral resistance F_{pt} on the pile section is equal to the passive force F_p minus the active force F_a. The force F_a may be computed from Rankine's theory, using the minimum coefficient of active earth pressure. The passive force F_p may be computed from the geometry of the wedge, assuming the Mohr-Coulomb failure theory to be valid for cohesionless soil. By referring to Fig.4(a), it can be seen that the shape of the wedge is defined by the pile diameter *d*, the depth of the wedge H=X, and by the angles α and β. It is assumed that no frictional resistance occurs on the base of the pile; therefore, there is no tangential force on the surface CDEF. The normal force F_n on planes ADE and BCF can be computed using a coefficient for the lateral earth pressure at rest. If the force F_n is known, the force F_s can be computed using Mohr-Coulomb theory.

Referring to Fig.4(b), the direction of the force F_Φ on the plane AEFB is known from theory; that is, the force acts at the angle Φ is the angle of internal friction of the cohesionless soil. The weight of the wedge *W* can be computed from the unit weight of the cohesionless soil γ. For cohesionless soil below the water table, the submerged unit weight should be used, of course. With the above information, the force $F_t$can be computed using the equations of statics. Therefore, the soil resistance F_{gt} against the pile may be computed as indicated previously. The lateral soil resistance per unit length of the pile at any depth may be found by differentiating the force F_{pt} with respect to the depth H=X. The result of that differentiation is shown in Fig.5.

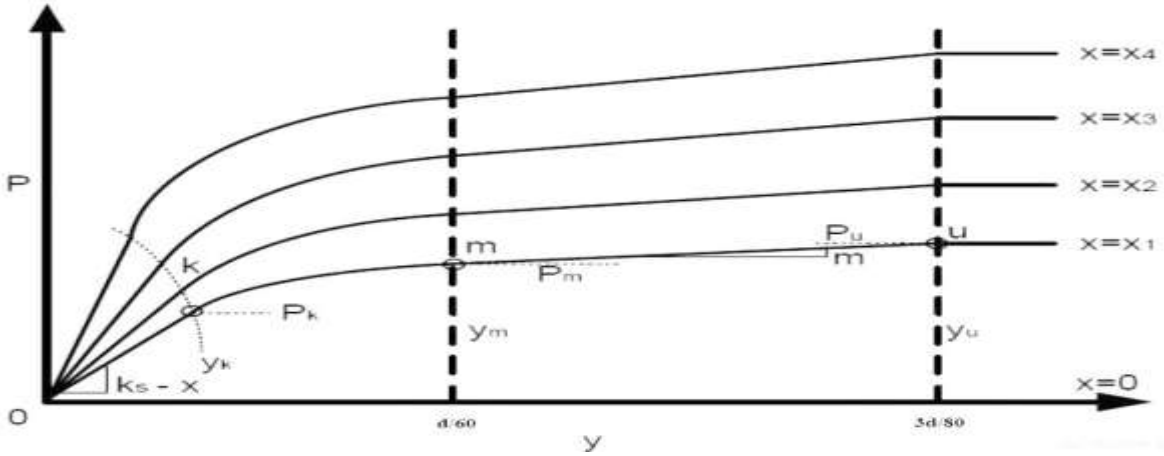

Fig.5 Construction of p-y curve

$$p_{st} = \gamma X\left[\frac{K_0 X \tan\phi\sin\beta}{\tan(\beta-\phi)\cos\alpha} + \frac{\tan\beta}{\tan(\beta-\phi)}(d + X\tan\beta\tan\alpha) + K_0 X\tan\beta(\tan\phi\sin\beta - \tan\alpha) - K_a d\right] \text{----(5)}$$

The values of the parameters in Fig.5 can be determined from theory and experimental data. The angle β is approximated by the following equation:

$$\beta = 45 + \phi/2 \quad \text{----------(6)}$$

This value for β is that which would be obtained from Rankine's theory for the passive pressure condition and for the two-dimensional case. The Rankine's conditions are not satisfied; however, some model experiments indicate that Eq.6 gives a fairly good approximation of the slope of the failure surface.

Values of the angle α have been determined from results of model tests with a small flat plate in cohesionless soil. From these model tests, Bowman [13] states that α is probably a function of the void ratio of the cohesionless soil, with values ranging from Φ/3 to Φ/2 for loose cohesionless soil to Φ for dense cohesionlesssoi.

Measurements at the soil surface around laterally loaded tubular model piles gave values for α as high as the value of Φ for dense cohesionless soil. Contours of the wedge that formed in front of the test piles at Verda River cohesionless soil indicated that the value of α was equal to about Φ/3 for static loading and about 3Φ/4 for cyclic loading.

The value of the coefficient of earth pressure at rest is dependent on the void ratio or relative density of the cohesionless soil and the process by which the deposit was formed. Terzaghi and Peck [14] state that the value of the coefficient of earth pressure at rest is about 0.4 for loose cohesionless soil and about 0.5 for dense cohesionless soil. In the absence of practice methods for determining relative density in the field, especially when soil deformations are large, a value of 0.4 for K_0 was selected in computing the ultimate lateral soil resistance near the ground surface. The value of α selected for this computation was Φ/2. The angle of internal friction Φ was taken as 3 degrees as indicated previously.

The coefficient K_a in Eq.5 is the Rankine's coefficient of minimum active earth pressure and is given by the following equation.

$$K_a = \tan^2(45 - \phi/2) \quad \text{----------(7)}$$

With regard to the use of theory or computing the ultimate lateral soil resistance against the pile at a considerable depth below the ground surface, the model shown in Fig.4 is employed. In this model, the soil is assumed to flow in the horizontal direction only. Referring to the model, Block 1will fail by shearing along the dashed lines allowing the soil in that block to follow the pile. Block 2 will fail along the dashed line as shown. Block 3 will slide horizontally. Block 4 will fail as shown, and Block 5 will be in the failure condition as the pile pushes against it. In this simplified model it is assumed that the cylindrical pile can be simulated by a rigid block of material.

With regard to the stress σ_1 at the block of the pile. It is reasoned that this stress cannot be less than the minimum active earth pressure. Otherwise, the soil could slump from the ground surface with a vertical motion, which is expressly eliminated in the model which is selected. With a value of σ_1, the other stresses can be computed using Mohr-Coulomb theory. Using the model shown, the ultimate lateral soil resistance at a depth such that there is horizontal flow around the pile may be computed by Eq.8:

$$p_{cd} = K_a d\gamma X\left(\tan^8\beta - 1\right) + K_0 d\gamma X \tan\phi \tan^4\beta \quad \text{----------(8)}$$

For the Verda River cohesionless soil test, values of p_c were computed using Eq. 5 and 8. These values are shown plotted in Fig.6. The values of the parameters used in making the computations are as follows:

Φ=39degrees, α=Φ/2, K_0=0.4, γ=10.40kN/m^3 (submerged unit weight), β=45degrees+Φ/2, d=600mm, E_p=21000MPa.

The symbol X_L shown in Fig.6 defines the intersection of Eqs. 5 and 8.

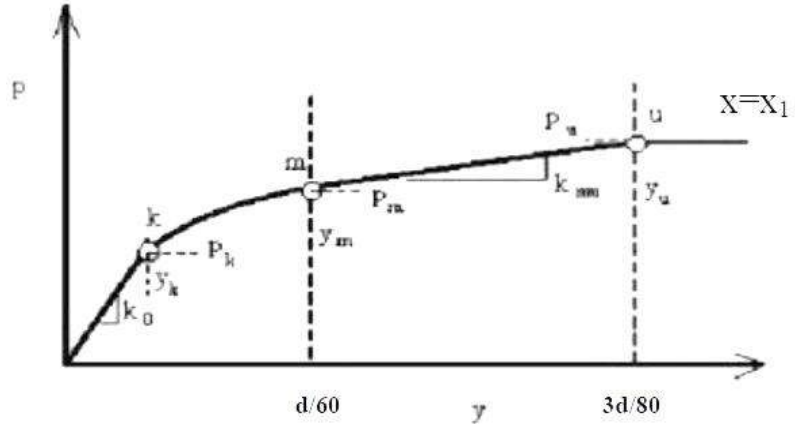

Fig.6 Construction of p-y curve

5.1 Recommended Procedure for Computing p-y Curves

A study of the families of *p-y* curves developed from the experiments both static and cyclic loading shows that the characteristic shape of the curves may be represented by the curves shown in Fig.7. The curves consist of three straight lines and a parabolic.

The initial straight portion of the *p-y* curve represents "elastic" behaviour of the cosionless soil and the horizontal portion of the curve represents "plastic behaviour". These two straight lines are joined with a parabola and a slopping straight line. The parabola and the intermediate straight line were selected empirically to yield a shape consistent with the experimental *p-y* curves.

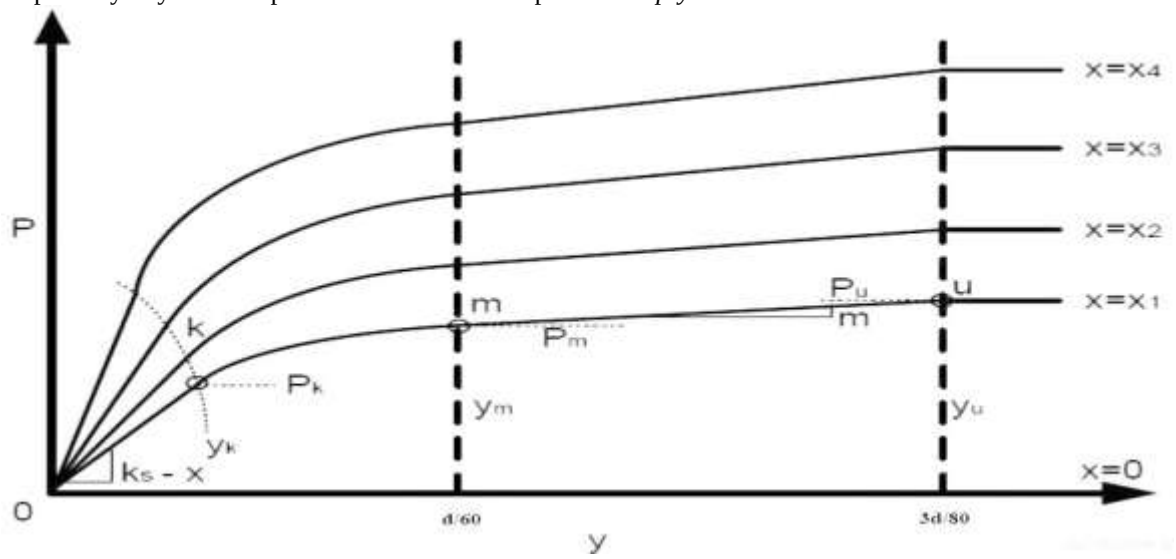

Fig.7 Ccharacteristic shape of a family of p-y curve for static and cyclic loadings in cohsionless soil.

The shape of the initial portion of the curves may be obtained from Table 2. The paragraphs below present the procedure for obtaining information for plotting the other portions of the curves.

When the computed values of ultimate lateral soil resistance were compared with the measured values. It was found that the agreement was poor. The poor agreement prevailed even though the effect of friction against the pile wall was considered and even though other parameters were varied through a reasonable range.

It was, therefore, decided to adjust the ultimate lateral soil resistance values according to the observed values, in the following manner:

$$p_u = Ap_c \quad \text{----------} \quad (9)$$

where, p_u=ultimate lateral soil resistance in proposed criteria in kN/m, p_c=ultimate lateral soil resistance from theory in kN/m, A=empirical adjustment factor.

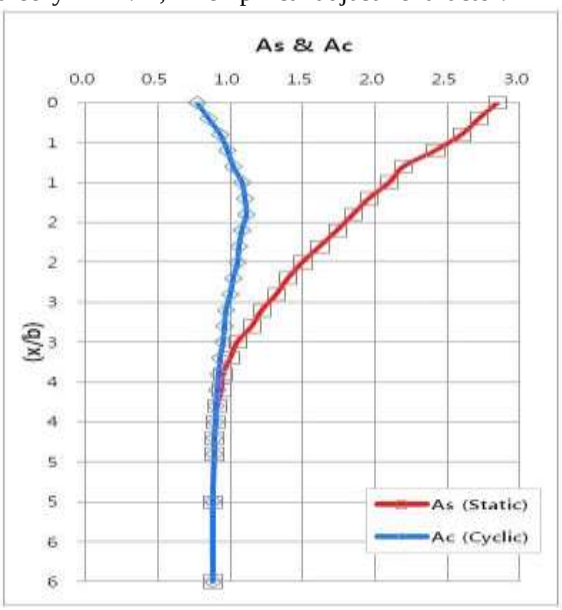

Fig.8 Values of coefficients As and Ac.

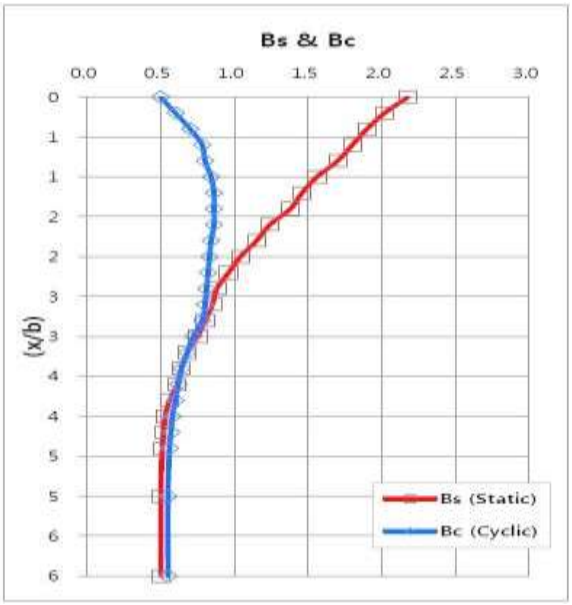

Fig.9 Values of coefficients Bs and Bc

Values of A were obtained by dividing the observed ultimate lateral soil resistance by the computed ultimate lateral soil resistance for the Verda River cohesionless soil tests. Values were obtained for A_s, the static case, and for A_c, the cyclic case. Plots of A_s and A_c various the non-dimensional depth x/b are shown in Fig.8. It should be noted again that observed values of ultimate lateral soil resistance were obtained to a relatively shallow depth. Eq.9, with values of A for either the static or the cyclic case, can be used to compute the ultimate lateral soil resistance to be used in the development of *p-y* curves.

In the preceding sections the magnitude of the ultimate lateral soil resistance and the slope of the initial straight line portion of the curve were obtained. It remains to establish values of *p* and *y* corresponding to points*k* and *m* as shown in Fig.7 and to establish the value of *y* corresponding to point *u*. These points define the intermediate portion of the *p-y* curves which can be represented by a parabola connecting points*k* and *m*.

For the results at Verda River cohesionless soil, it was found that the values of y_m and y_u were 0.01m and 0.022m, respectively. The respective values of y/d were 1/60 and 3/80.

The values of p_u was obtained from the *p-y* curves, for both static and cyclic loading. From these values, values of the parameter B were computed as follows:

$$B = \frac{p_m}{p_c} \quad \text{----------(10)}$$

Values of B for both the static and cyclic cases are shown in Fig.9. Thus, from the values of p_c, computed by Eq.5 or Eq.8, values of p_m can be obtained for any pile in any soil by using the empirical relationships which are given.

The *p-y* curve can now be completed by constructing a parabola between points*k* and *m*. This was accomplished by constructing a parabola, passing through the origin, and connecting at point *m* with a slope equal to that of the straight line from *m* to *u*. The intersection of this parabola with the initial straight line portion of the *p-y* curve established point *k*. This completes the specifications for the recommended family of *p-y* curves, both for static and cyclic loading.

For convenience in making computations for a family of *p-y* curves, the following step-by-step procedure is presented. A typical family of such curves is shown in Fig.7.

1. Obtain values for significant soil properties and pile dimensions, Φ, γ, and *d*.
2. Use the following for computing lateral soil resistance.

   α=Φ/2, β=45+Φ/2, K_o=0.4, and $K_a=\tan^2(45-\Phi/2)$.

3. Use the following equations for computing lateral soil resistance:

   a. Ultimate lateral soil resistance near ground surface,

$$p_{st} = \gamma X\left[\frac{K_0 X \tan\phi\sin\beta}{\tan(\beta-\phi)\cos\alpha} + \frac{\tan\beta}{\tan(\beta-\phi)}(d + X\tan\beta\tan\alpha) + K_0 X\tan\beta(\tan\phi\sin\beta - \tan\alpha) - K_a d\right] \text{----(5)}$$

   b. Ultimate lateral soil resistance well below the ground surface,

$$p_{cd} = K_a d\gamma X(\tan^8\beta - 1) + K_0 d\gamma X\tan\phi\tan^4\beta \quad \text{----------(9)}$$

4. Find the intersection, X_r, of the equations for the ultimate lateral soil resistance near ground surface and the ultimate lateral soil resitance well below the ground surface. Above this depth use Eq.5. Below this depth use Eq.8.
5. Select one depth at which a *p-y* curve is defined.
6. Establish y_u as 3d/80. Compute $p_u$by the following equation:

$$p_u = Ap_c \quad \text{----------(10)}$$

7. Establish ym as d/60. Compute pm by the following equation:

$$p_m = 8p_c \quad \text{----------(11}$$

Use the appropriate value of B from Fig.9, for the particular non-dimensional depth, and for either the static or cyclic case. Use the approporiate equation for p_c.

8. Establish the slope of the initial portion of the p-y curve by selecting the appropriate value of k

$p = Cy^{1/n}$ from Table 2.-- ----------(12)

9. Select the following parabola to be fitted between points*k* and *m*.

10. Fit the parabola between points k and m as follows:

a. Get slope of line between points*m* and *u* by,

$$m = \frac{p_u - p_m}{y_u - y_m} \quad \text{----------(13)}$$

b. Otain the power of the parabolic section by,

$$n = \frac{p_m}{m y_m} \quad \text{----------(14)}$$

c. Obtain the coefficient C as follows:

$$C = \frac{p_m}{y_m^{1/n}} \quad \text{----------(15)}$$

d. Determine poont*k* as,

$$y_k = \left(\frac{C}{kx}\right)^{n/n-1} \quad \text{----------(16)}$$

e. Compute appropriate number of points on the parabola by using Eq.12.

This completes the development of the *p-y* curve for the desired depth. Any number of curves can be developed by repeating the steps above or each depth desired.

Example: The example shown here is to use the above steps to reproduce the curves given by Reese and Impe[2001]. The soil and pile parameters are: Submerged medium dense sand: γ^i=9.8kN/m^3, Φ=35^0, N_h=16300kN/m^3.

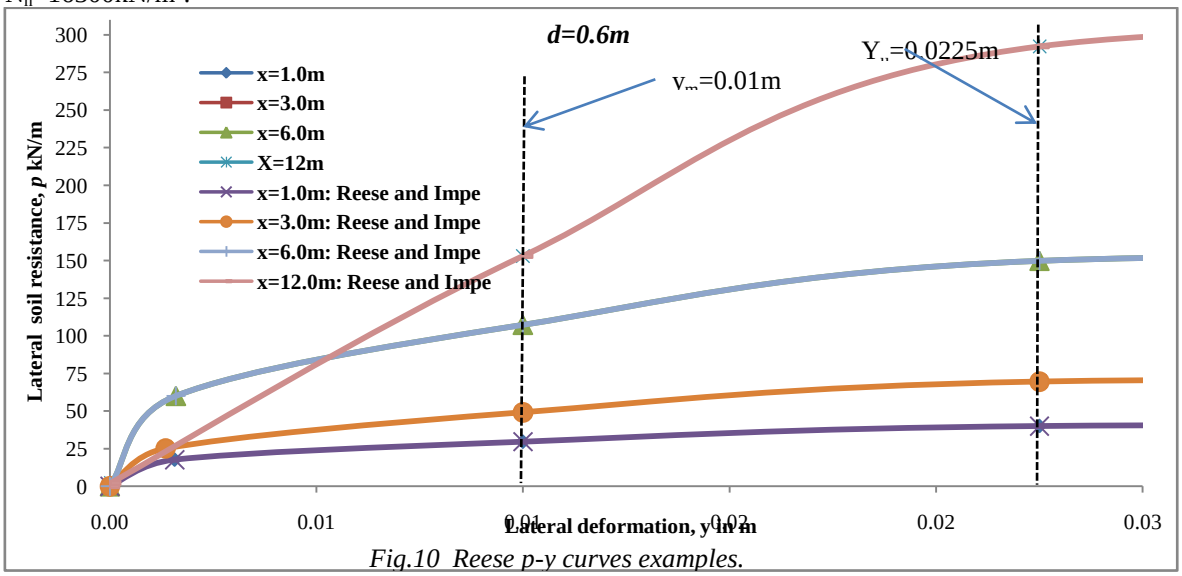

Fig.10 Reese p-y curves examples.

5.2 Parametric study.

Although soil submerged density, lateral soil modulus variation, angle of internal friction and pile diameter are correlated, a parametric study was conducted to examine the effects of each single parameter on *p-y* curves. The effects of pile diameter were also investigated.

When conducting parametric study, the *p-y* curves at 1.875m depth were plotted using the values of the basic parameters as below for static and cyclic loading test:Soil properties: γ^i=10.40kN/m^3, N_h=30000kN/m^3, Φ=39^0, pile diameter=0.6m.

5.3 Effects of angle of internal friction (Φ).

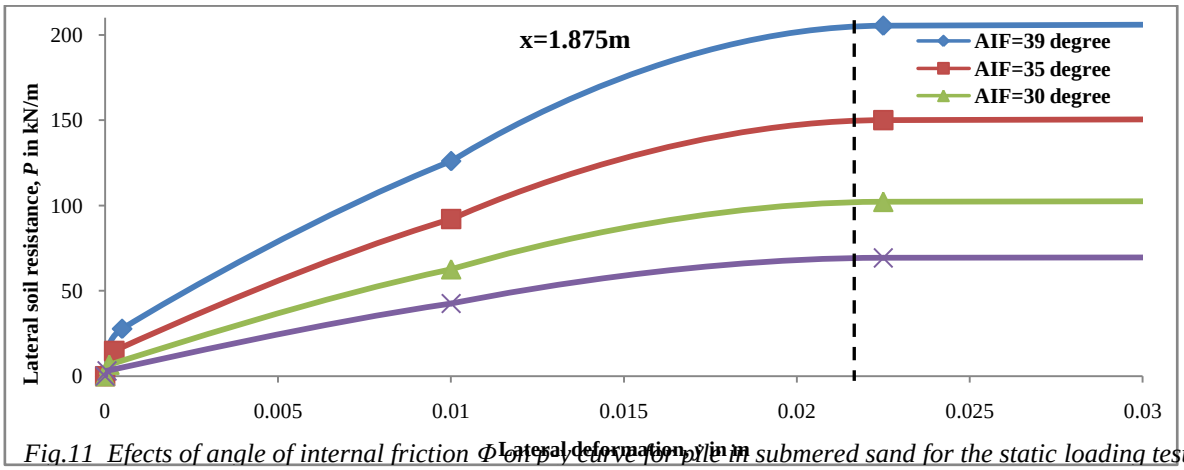

Fig.11 Efects of angle of internal friction Φ on p-y curve for pile in submered sand for the static loading test.

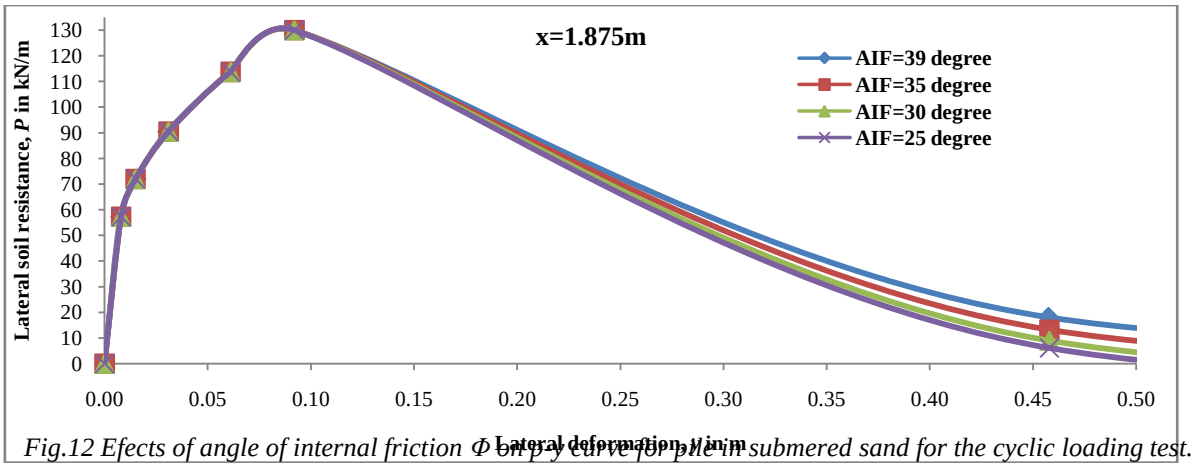

Fig.12 Efects of angle of internal friction Φ on p-y curve for pile in submered sand for the cyclic loading test.

Figure 11 to 12 shows the effects of angle of internal friction Φ on p-y curve. It can be seen that as angle of internal friction Φ increases rom 25^0 to 39^0, *p-y* curves at 1.875m depth vary a lot. Thereore, angle of internal friction Φ has significant effects on p-y curve.

5.4 Effects of submerged density(γ^i).

Figure 13 to 14 shows the effects of submerged density γ^i on *p-y* curve. It can e seen that as submerged density γ^iincreases from 10.40 to 20.00kN/m3, *p-y* curves at 1.875m depth vary lot. Therefore, submerged density γ^i has significant effects on p-y curve.

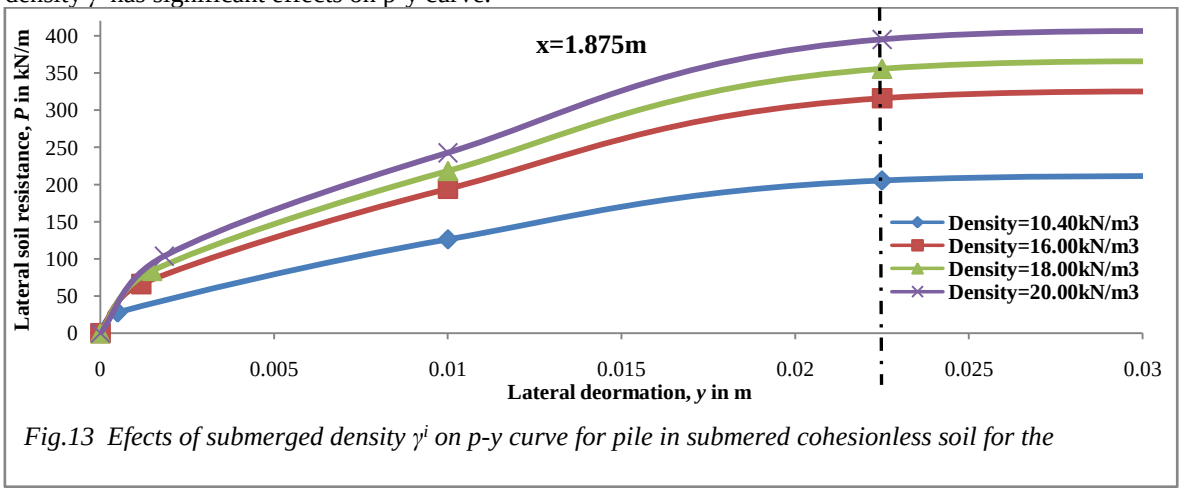

Fig.13 Efects of submerged density γ^i on p-y curve for pile in submered cohesionless soil for the

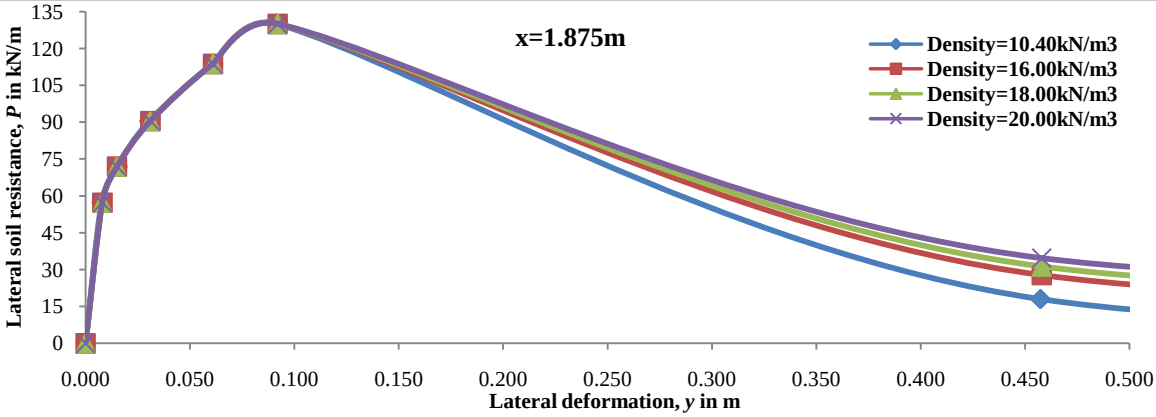

Fig.14 Efects of submerged density γ^i on p-y curve for pile in submered cohesioness soil for the cyclic loading test.

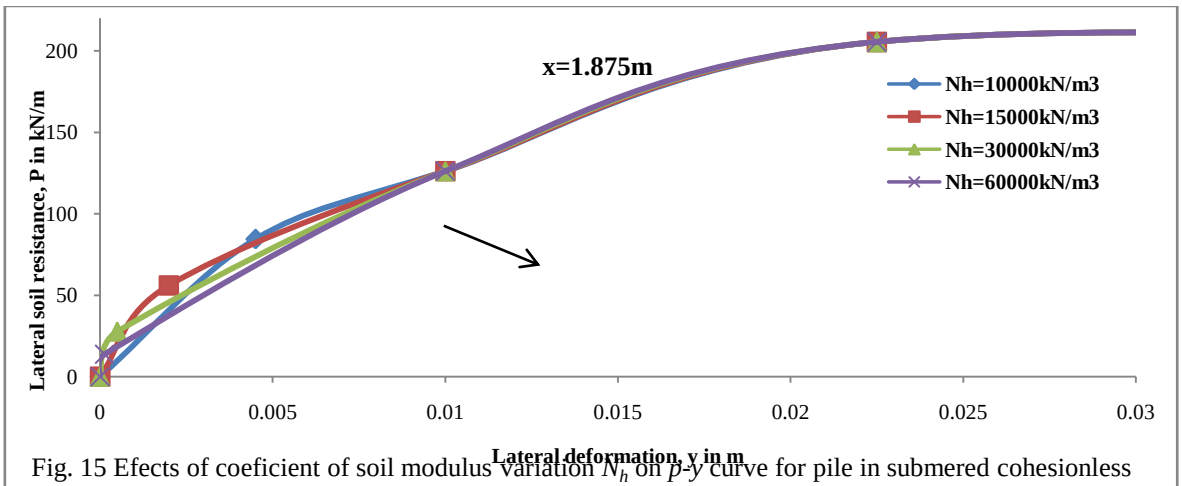

Fig. 15 Efects of coeficient of soil modulus variation N_h on *p-y* curve for pile in submered cohesionless soil for the static loading test.

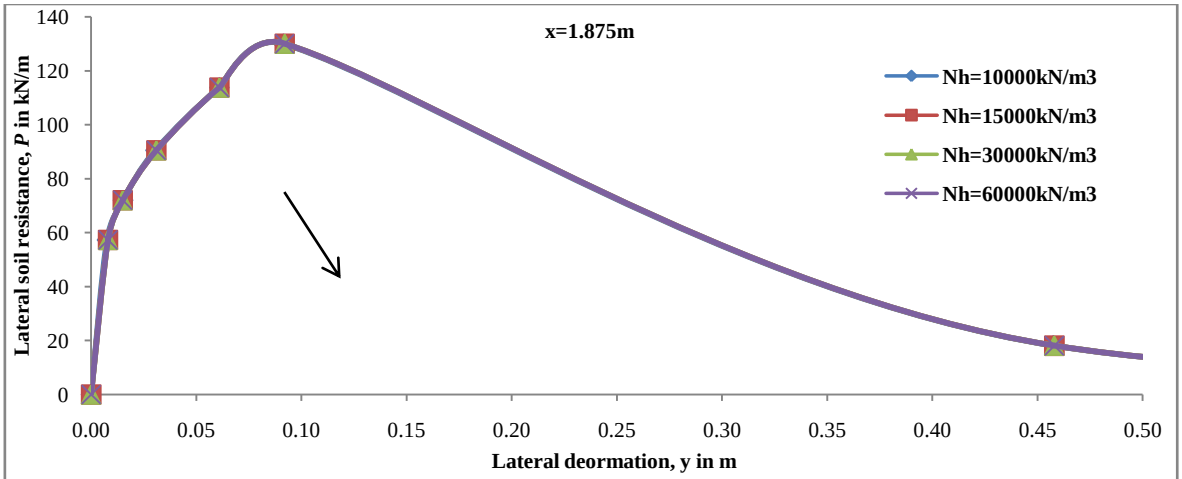

Fig.16 Efects of coeficient of soil modulus variation N_h on p-y curve for pile in submered cohesionless soil for the cyclic loading test.

Figure 15 and 16 shows the effects of coefficient of soil modulus variation $N_h$on *p-y* curve. It can be seen that as coefficient of soil modulus variation increases from 10000 to 60000kN/m^3, *p-y* curves at 1.875m depth vary only a small amount. Thereore, coefficient of soil modulus variation N_h has no significant effects on p-y curve.

5.4Efects of pile diameter *(d)*.

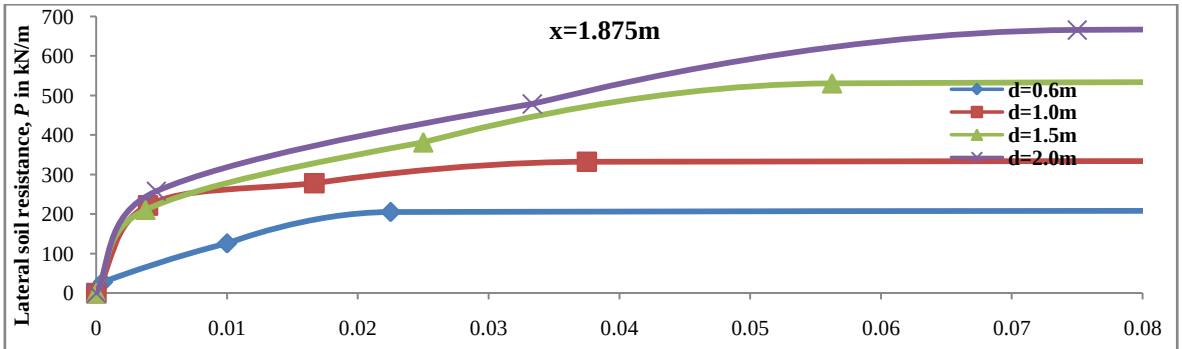

Fig.17 Efects of pile diameter variation d on p-y curve for pile in sumerged cohesionless soil for the static loading test.

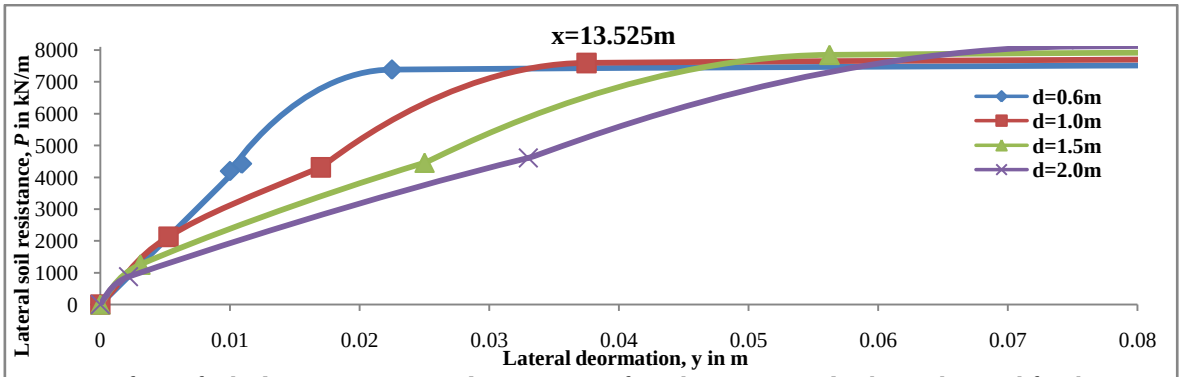

Fig.18 Efects of pile diameter variation d on p-y curve for pile in sumerged cohesionless soil for the static loading test.

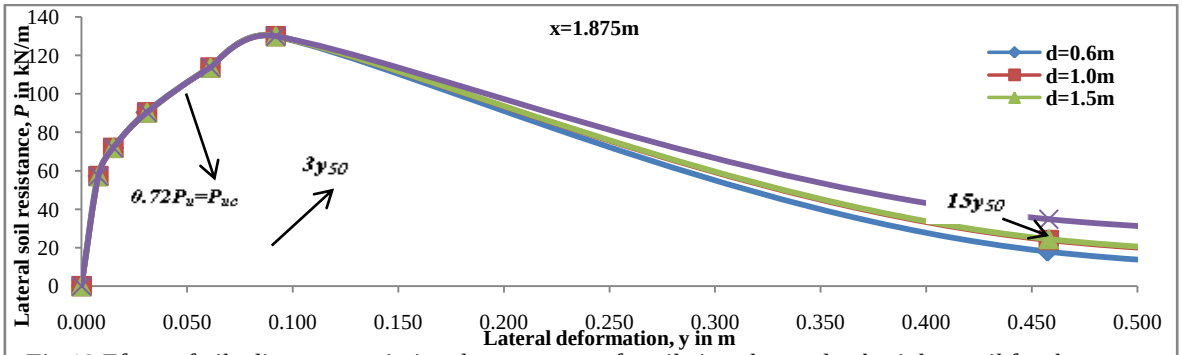

Fig.19 Efects of pile diameter variation d on p-y curve for pile in submered cohesinless soil for the cyclic loading test.

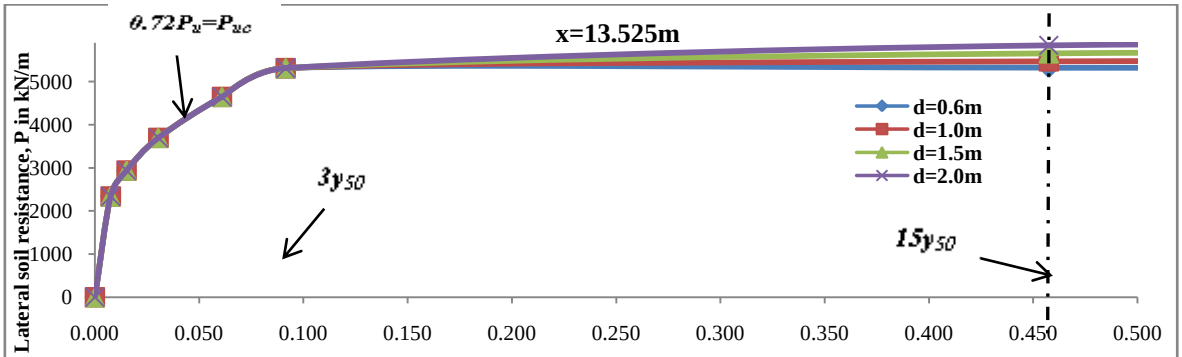

Fig. 20 Efects of pile diameter variation d on p-y curve for pile in submered cohesionless soil for the cyclic loading test.

Figure 17 to 20 shows the effects of pile diameter *d* on *p-y* curve for both static and cyclic loading test. It can be seen that as pile diameter *d* increases from 0.6m to 2.0m, the slope of the initial segment of the *p-y* curves the same depth keep the same. The slope increases as depth goes deeper. It also can be seen that the lateral soil resistance increases as pile diameter increases. This is due to th fact that more soil was involved to resist pile deformation as pile diameter increases.

The interesting thing is that the middle part of the *p-y* curves at 13.525m depth (Fig.18 and 20) displays opposite diameter effects from those at 1.875m depth (Fig.17 and 19). At 1.875m depth (Fig.17 and 19) lateral soil resistance in the middle part of the *p-y* curves increases as increasing pile diameter, while at 13.525m depth (Fig.18 and 20) lateral soil resistance decreases as increasing pile diameter, while at 13.525m depth (Fig.18 and 20) lateral soil resistance decreases as increasing pile diameter. This may be due to the diferent soil failure modes at different depth. At 1.875m depth soil fails following the wedge failure mode (Fig.4(a)), while at 13.525m depth soil fails following the lock failure mode (Fig.4(b)).

6. Comparision Between Empirical and Computed Results Using Proposed Method.

A computer program (*SoilWorks 2D FEM*) was developed to allow comparision of values of moment, deformation, slope and coefficient of soil modulus variation so that comparisions can be made with values measured in the field.

The model is a single pile subjected a lateral load at the pile head. The soil layer is uniform cohesionless soil with water table at the pile head. The pile has a diameter of 0.6m and a height of 13.525m. The objective of the *SoilWorks 2D FEM* software runs performed is to study the effects of the soil properties (angle of internal friction Φ, submerged density γ^i and coefficient of soil modulus variation N_h) on the behaviour of Reese cohesionless soil model. Note that the above mentioned soil properties are dependent with each other in reality. One may not change some of them and keep the other constant. However, in order to study the behaviour of the Reese cohesionless soil model in *SoilWorks 2D FEM* program, we did the following runs (changing one and keeping the other two constant).

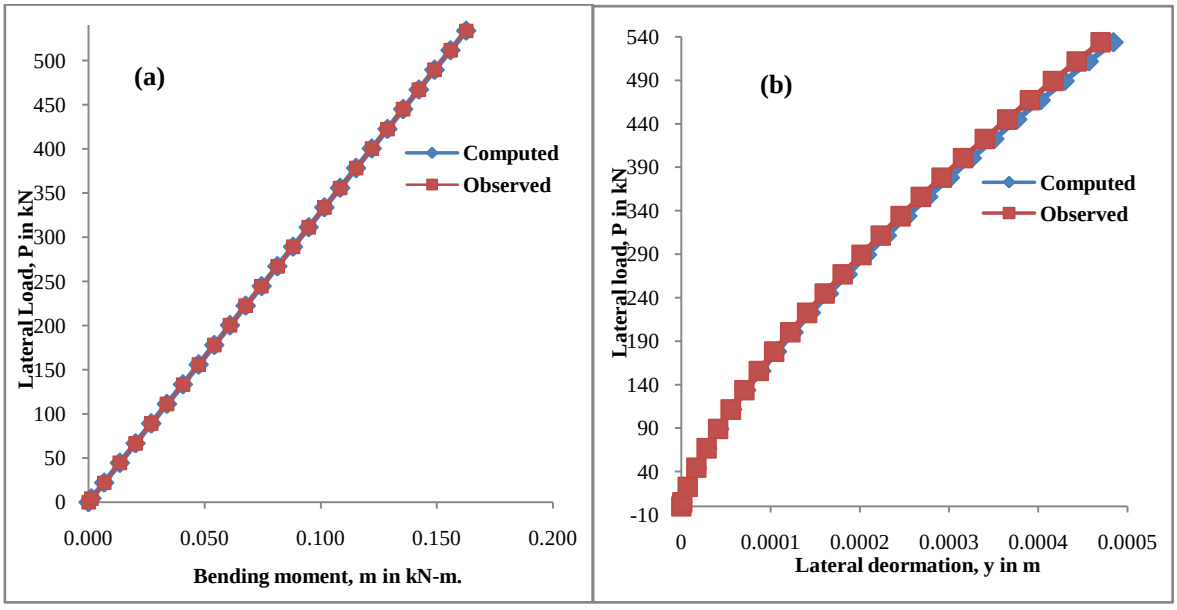

Fig.21 Lateral load versus maximum moment (a) and lateral deformation (b) at the ground line for a model pile in cohesionless soil.

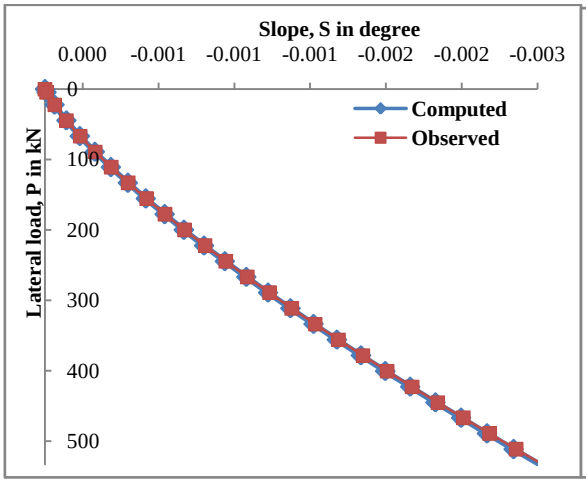

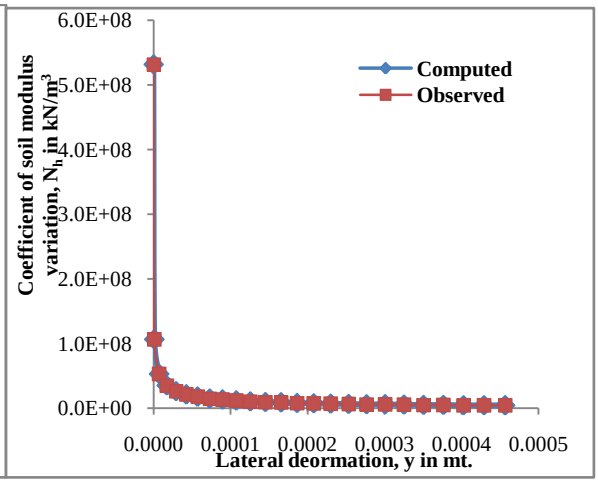

Fig.22 Lateral load versus slope at the ground line for a model pile in cohesionless soil.

Fig.23 Coefficient of soil modulus variation versus lateral deformation at the ground line for a model pile in sand.

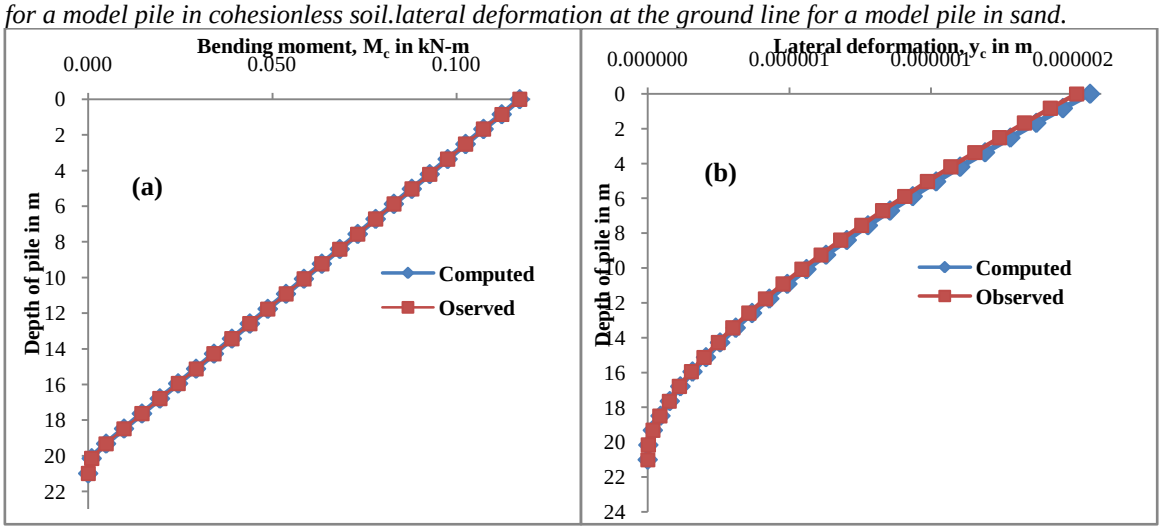

Fig.24 Length of pile versus bending moment (a) and lateral deormation (b) at the ground line for a model pile of cyclic load test incohesionless soil.

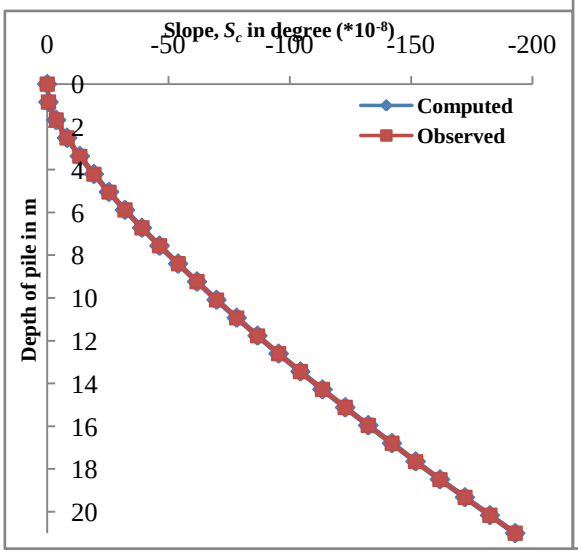

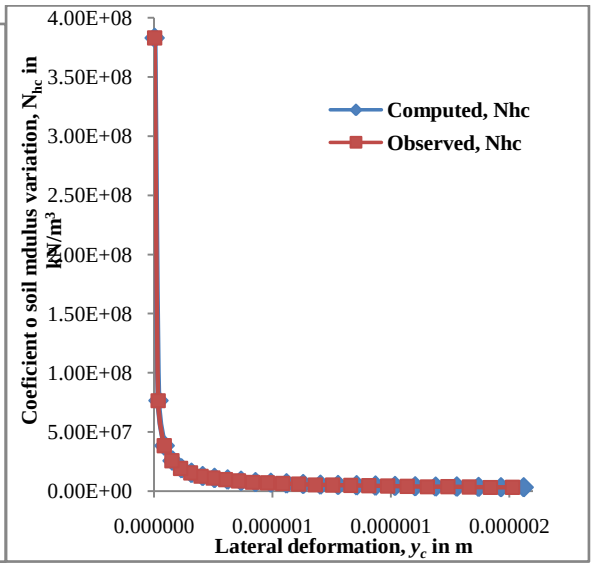

Fig.25 Slope versus length of pile at the ground line for a model pile of cyclic test in sand.

Fig. 26 Coefficient of soil modulus variation versus lateral deformation at the ground line for a model pile

of cyclic load test in sand.

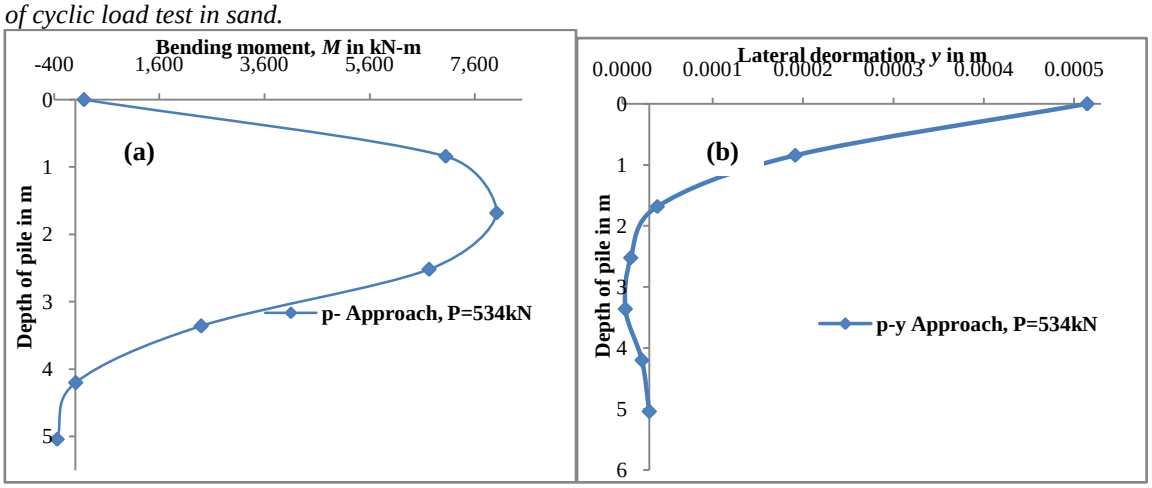

Fig.27 Depth of pile versus bending moment (a) and lateral deformation at maximum load of a model pile in cohesionless soil.

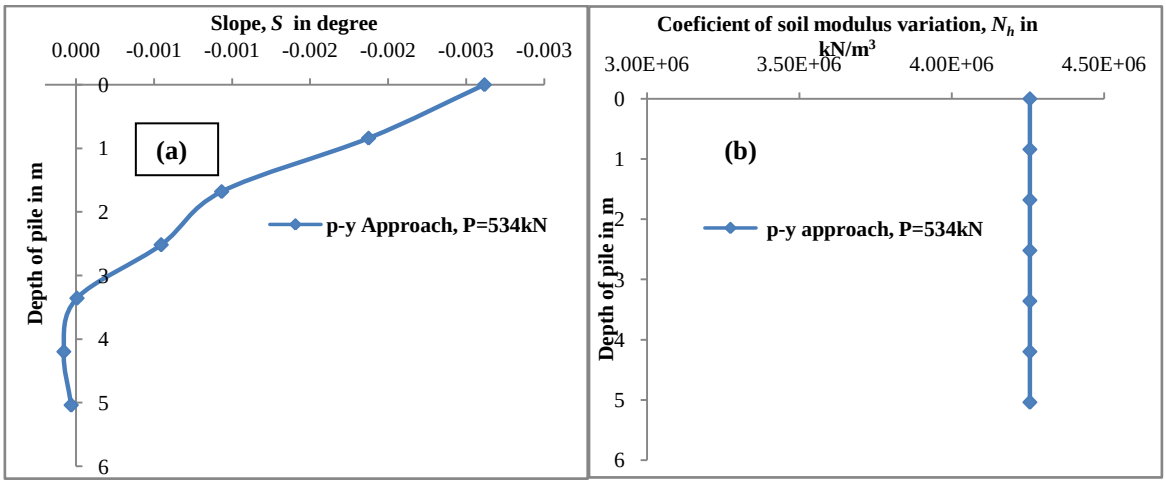

Fig. 28 Depth of pile versus slope (a) and coefficient of soil modulus variation (b) at maxumum load of a model pile in cohesionless soil.

Measured and computed values of lateral load versus maximum bending moment for the static test are shown in Fig.21(a). Lateral load versus measured and computed values of lateral deformation at the ground line is shown in Fig.21(b) and versus slope at the ground line is shown in Fig.22 and versus coefficient of soil modulus variation at the ground line is shown in Fig.23 for the static case. Similar plots are shown for cyclic loading in Figs.24through 26. In addition to the comparision shown above, *p-y* approach curves are shown for the maximum load, in Fig.27 and Fig.28 for the static test along the depth of pile.

It can be seen that the above figures, the bending moment increases as the depth of pile and lateral load increases. This is due to the fact that more soil was involved to resist the pile lateral deformation as lateral load increases.

The interesting thing is that the *p-y* approach at 1.68m depth Fig.27(a), bending moment increases as increasing the lateral load, while at 4.2m depth bending moment decreases as increasing lateral load. This is may be due to the different soil failure modes at diferent depth. At 1.68m depth soil fails following the wedge failure mode (Fig.4a), while at 4.2m depth soil fails following the block failure mode (Fig.4b).

Figure 27(b) shows that the effect of lateral loads on *p-y* curve. It can be seen that as lateral loads increases from 0.0 to 534kN, *p-y* approach at 1.68m depth vary only a small amount. Therefore, lateral load *P* has no significant effects on *p-y* approach.

The non-linear portion will have larger soil resistance when lateral load increases at shallow depth. The soil resistance at non-linear portion will decrease at certain depth as lateral load increases. This model is good for driven piles in cohesionless soil below or above water table.

The agreements between the measured and computed values in all cases are agreement up to about *P*= 440kN, and beyond this load, the observed values are greater than the computed by about 5% which is expected since the soil yields at a load higher than 440kN at this stage and there is a plastic flow beyond this load and indicating that the recommendations for the *p-y* curves in cohesionless soil are valid at least for the Verda River cohesoinless soil tests. All the known parameters which influence the problem are included in the recommendations, allowing the recommendations to be applied to the analysis of any laterally loaded piles in cohesionless soil.

6.1 Effect of the lateral soil modulus variation N_h.

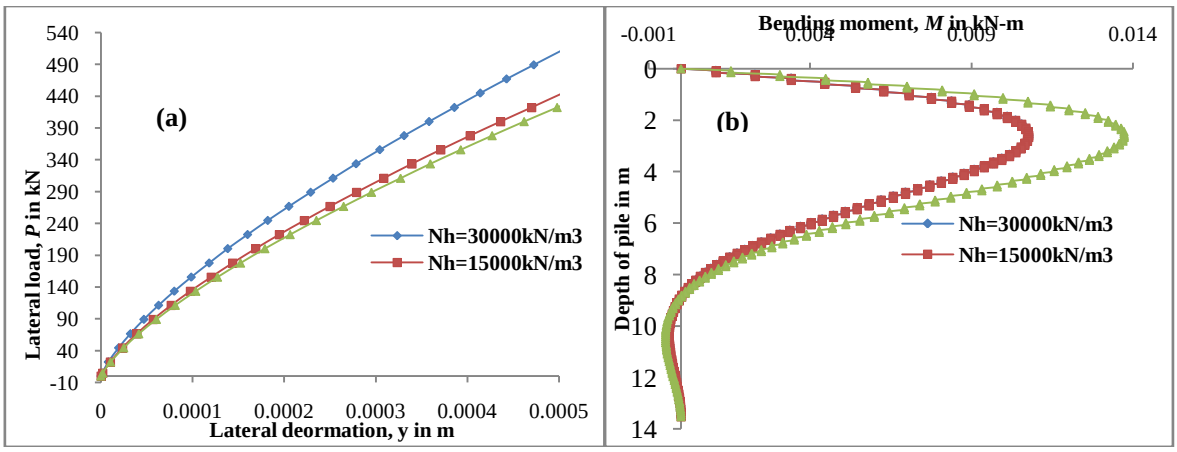

Fig. 29 Lateral load versus lateral deformation (a) and bending moment distribution (b) for different coefficient of soil modulus variation $N_h$of a model pile in cohesionless soil.

Figure 29(a) and (b) shows the lateral load versus lateral deformation and the bending moment distribution of the pile for the coefficient of soil modulus variation(10000, 15000 and 30000kN/m^3), while keeping the angle of internal friction 35 degrees, and the submerged density 16.00kN/m^3) .

It is noted that the curves for the coefficient of soil modulus variation=15000 and 30000kN/m^3 are almost the same. This should not happen in reality since only the coefficient of soil modulus variation is changed here.

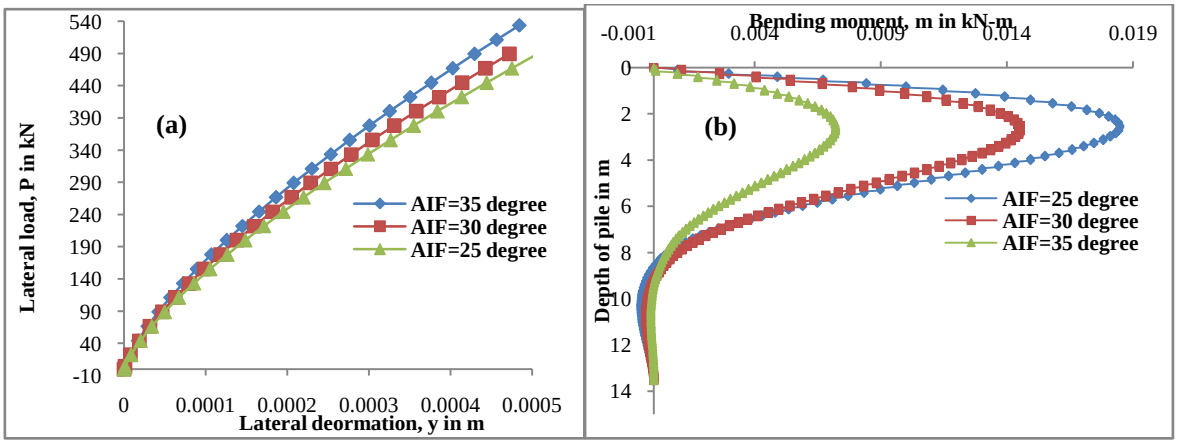

Fig. 30 Lateral load versus lateral deformation (a) and bending moment distribution (b) for differen angle of internal friction Φof a model pile in cohesionless soil.

Figure 30(a) and (b) shows the lateral load versus lateral deformation and the bending moment distribution of the pile for the angle of internal friction(35, 30 and 25 degrees), while keeping the coefficient of soil modulus variation 10000 kN/m^3 and the submerged density 16.00kN/m^3.

It is noted that the curves for the angle of internal friction Φ increase from 25 degree to 35 degree, lateral deformation and bending moment decreases. This is due to the fact that more soil was involved to resist the pile lateral deformation as angle of internal friction Φ increases.

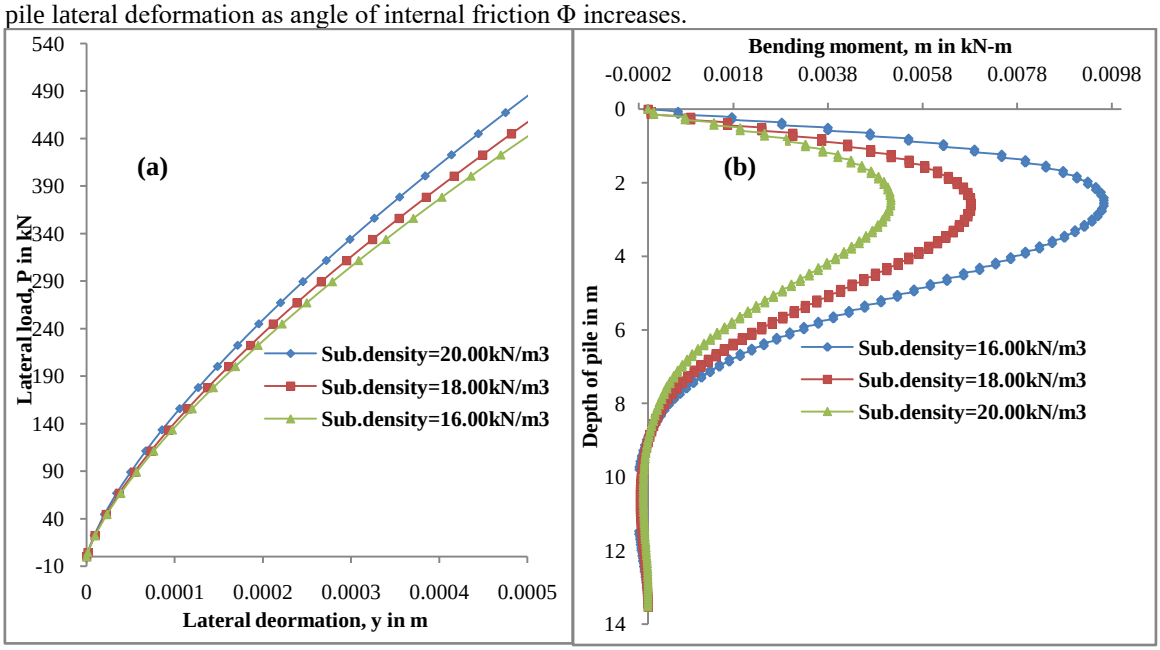

Fig. 31 Lateral load versus lateral deformation (a) and bending moment distribution (b) for different sumerged density γ^i of a model pile in cohesionless soil.

Figure 31 (a) and (b) shows the lateral deformation and the bending moment distribution of the pile for different submerged densities (16.00, 18.00 and 20.00kN/m^3), while keeping the angle of internal friction 25 degree and the coefficient of soil modulus variation N_h=10000kN/m^3.

It is noted that the curves for the submerged density γ^i increase from 16.00kN/m^3 to 20.00kN/m^3, lateral deformation and bending moment (at 2.26m) decreases. This is due to the fact that more soil was involved to resist the pile lateral deformation as submerged density γ^i increases.

6.2 Assumptions and Limitations Concerning the Proposed Method

1. The soil is assumed to be cohesionless soil. A soil which is predominantly granular but contains a sufficient amount of clay to give some cohesion would behave entirely differently than cohesionless soil.

2. The pile is assumed to have been driven so that the cohesionless soil is densified rather than loosened during installation. The proposed method does not apply to piles that have been installed by jetting.

3. The pile is assumed to be essentially vertical. However, it is believed that the method can be used to predict the behaviour of batter piles if the batter is not too severe.

6.3 Erosion

The above recommendations are for a known position of the groundline. While a consideration of erosion is not a part of this research program, it should be mentioned that experience and theory show that cohesionless soil around an offshore structure will normally be subjected to severe occur. Several meter of soil may be removed. Such a condition must be prevented or taken into account in the analysis.

7. Conclussions

Following conclusions may be drawn from the study.

1. The proposed method for predicting *p-y* curves or laterally loaded piles in cohesionless soil involves the use of the parameters which are believed to be important and employs available theories or predicting soil behaviour. Predictions of the behaviour of the Verda River cohesionless soil, piles, using *p-y* curves developed by the proposed method, agree very well with the experiments. Further, studies of five additional experiments reported in technical literature [4,15,16,17,18] show that the proposed method gives reasonable agreement with those experiments or is somewhat conservatives.
2. The above facts appear to confirm the validity of the proposed method; however, the method makes liberal use of empirical coefficients derived from the Verda River cohesionless soil tests. Evidence in geotechnical literature amply declares that each cohesionless soil deposit is distinctive, with characteristics depending not only on the nature of the grains and their arrangement but also on the history of the deposit. Therefore, the writers urge that the method be used with caution and judgement.
3 Concerning the care which should be exercised in predicting the behaviour of piles under lateral loading, mention should be made of the solution of Eq.1. While a discussion of numerical techniques employed in the solution of the equation is beyond the scope of this paper, the writers should report that their experiences indicate that serious errors can be made by inexperienced analysis.
4. Finally, it should be noted that the proposed method does not include a factor of safety for a particular design is a problem unique to that design.
5. The non-linear portion will have larger lateral soil resistance when pile diameter increases at shallow depth. The lateral soil resistance at non-linear portion will decrease at certain depth as pile diameter increases.
6. The effects of each parameter are uncertain when considered alone. The angle of internal friction, coefficient of soil modulus variation, and submerged density are correlated with each other.

References

1. Terzaghi, Karl, Evaluation of Coefficients of Subgrade Reaction, *Geotechnic, Vol.5, Issue 5*, December, 1995, 297-326.
2. Parker, Frazier and Lymon C. Reese, Lateral Pile-Soil Interaction Curves for Sand, Proceedings, The International Symposium on the Engineering Properties of Sea-Floor Soils and Their Geophysical Indentification, University of Washington, Seattle, Washington, July 25, 1971.
3. Hetenyl.M., Beams on Elastic Foundation, University of Michigan Press, Ann Arbor, Michigan, 1945.
4. Glaser, Sol M., Lateral Load Tests on Vertical Fixed-head and Free-head Piles, *Special Technical Publishing 154, American Society for Testing Materials*,1953,p.75.
5. Reese, Lymon C. and Hudson Matlock, Non-Dimensional Solutionss for Laterally Loaded Piles with Soil Modulus Assumed Proportional to Depth, Proceedings, *Eight Texas Confernce on Soil Mechanics and Foundation Engineering*, Austin, Texas, 1956.
6. Matlock, Hudson and Lymon C. Reese, Generalized Solutions for Laterally Loaded Piles, Journal of the Soil Mechanics and Foundations Division, *American Society of Civil Engineers*, October, 1960, p.63.
7. Matlock, Hudson and Lymon C. Reese, Foundation Analysis of Offshore Pile-Supported Structures, Proceedings, Fifth International Conference, *International Society of Soil Mechanics and Foundation Engineering, Paris, Vol.2*, 1961, p.91.
8. Matlock, Hudson, Correlations for Design of Laterally Loaded Piles in Soft Clay, *Presented at the Second Annual offshore Technology Conference*, Houston, Texas, 1970.
9. McClelland, Bramlette and J.A.Focht, Jr.Soil Modulus of Laterally Loaded Piles, *Transactions, American Society of Civil Engineers, Vol.123*, 1071-74.
10. Reese, Lymon C, and William R.Cox, Soil Behaviour from Analysis of Tests of Uninstrumented Piles Under Lateral Loading, Performance of Deep Foundation, *ASTM STP 444, American Society of Civil Engineers, Vol.123*, 161-76.

11. Cox. William R., LymonC.Reese, and Berry R. Grubbs, Field Testing of Laterally Loaded Piles in Sand, *Sixth Annual Offshore Technology Conference*, Huston, Texas, 1974.
12. Matlock, Hudson and E.A.Ripperger, Procedures and Instrumentation for Tests on a Laterally Loaded Pile, *Proceedings, Eight Texas Conference on Soil Mechanics and Foundation Engineering*, Auston, Texas, 1956.
13. Bowman, Elliott R., Investigation of the Lateral Resistance to Movement of a Plate in Cohesionless Soil, Unpulished Master's Thesis, Austin, The University of Texas, January, 1958.
14. Terzaghi.Karl. and Ralph B.Peck, Soil Mechanics in Engineering Practice, John Wiley and Sons. Inc.New York, 19448, p.140.
15. Fruce and Associates, Pile Driving and Loading Tests, Report to Corps of Engineers, Little Rock, Atkansas, on Arkansas River Tests, September, 1964.
16. Masam.H.G., and J.A.Bishop, Measurement of Earth Pressure and Deflection Along the Embedded Portion of a 40-ft. Steel Pile, Symposium on Lateral Load Tests on Piles, *American Society for Testing and Materials, Special Technical Publication No.154-A*, June,1953, 1-21.
17. Reese.Lymon C., Preliminary Results on Lateral Load Tests on Vertical Piles at Padre Island, *Report to Production Technical Services Division, Shell Oil Company*, Houston, Texas, May, 1958 (unpublished).
18. Wagner,A.A., Lateral-Load Tests on Piles for Design Information, Symposium on Lateral Load Tests on Piles, *American Society for Testing and Materials, Special Technical Publication No.154*, July,1953, 59-74.
19. K. Byung-Tak, K. Young-Su,Back analysis for prediction and behaviour of laterally loaded single piles in sand, *KSCE journal of civil engineering*, ***3 Issue 3***, September 1999, 273-288.
20. S. Prakash, Sanjeevkumar,Nonlinear lateral pile deflection prediction in sand, *Journal of Geotech. Eng. ASCE, **122 Issue 2***, 1996, 130-138.
21. S.S. Chandrasekaran, A. Boominathan, G.R. Dodagoudar, Group interaction effects on laterally loaded piles in clay, *Journal of Geotech. andGeoen. Eng.**130 Issue 4,***2010, 573-582.
22. R. Sundaravadivelu, K. Muthukkumaran, S. Gandhi, Effect of slope on p-y curves due to surcharge load, *Soils Found.*,**48 Issue 3**, 2008, 353–361.
23. D. Rathod, K. Muthukkumaran, T.G. Sitharam, Effect of slope on p-y curves for laterally loaded piles in soft clay, *J. Geotech. Geologi. Eng. 2017,*1-16.